Supplementary Information

"Poly(ADP-ribose) glycohydrolase coordinates meiotic DNA double-strand break induction and repair independent of its catalytic activity"

Janisiw et al.

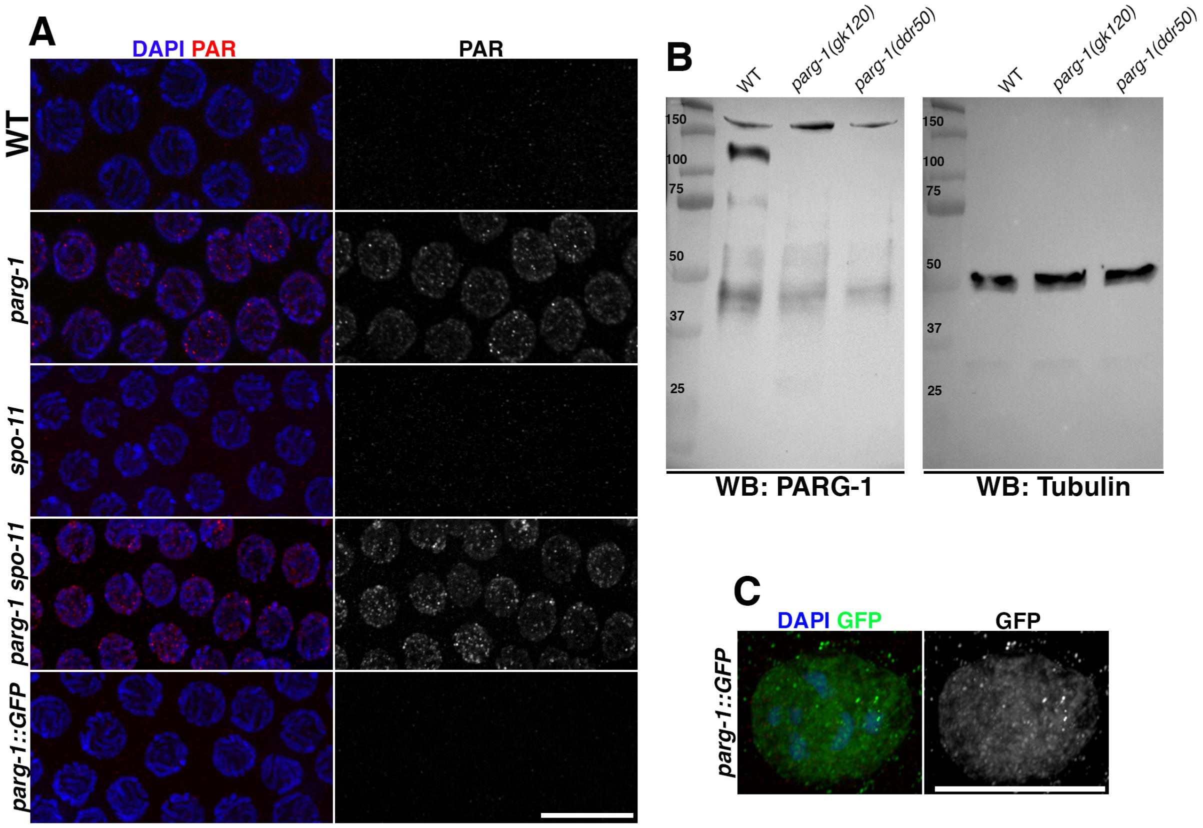

Supplementary Figure 1. PAR accumulates in absence of endogenous DSBs. (A) Immunostaining analysis showing accumulation of PAR in *parg-1* mutants even in absence of SPO-11-induced DSBs. *parg-1::GFP* does not accumulate PAR, indicating functionality of the fusion protein. Scale bar 10 μm. Analysis was performed in biological duplicates. **(B)** Western blot with anti-PARG-1 antibody on whole cell extract in WT, *parg-1(gk120)* and *parg-1(ddr50)*, showing that *parg-1* mutants are null. Tubulin was used as loading control. Analysis was performed in biological duplicates. **(C)** Representative image of a diakinesis nucleus from *parg-1::GFP* worms displaying mostly nucleoplasmic localization. Scale bar 5 μm. Analysis was performed in biological duplicates.

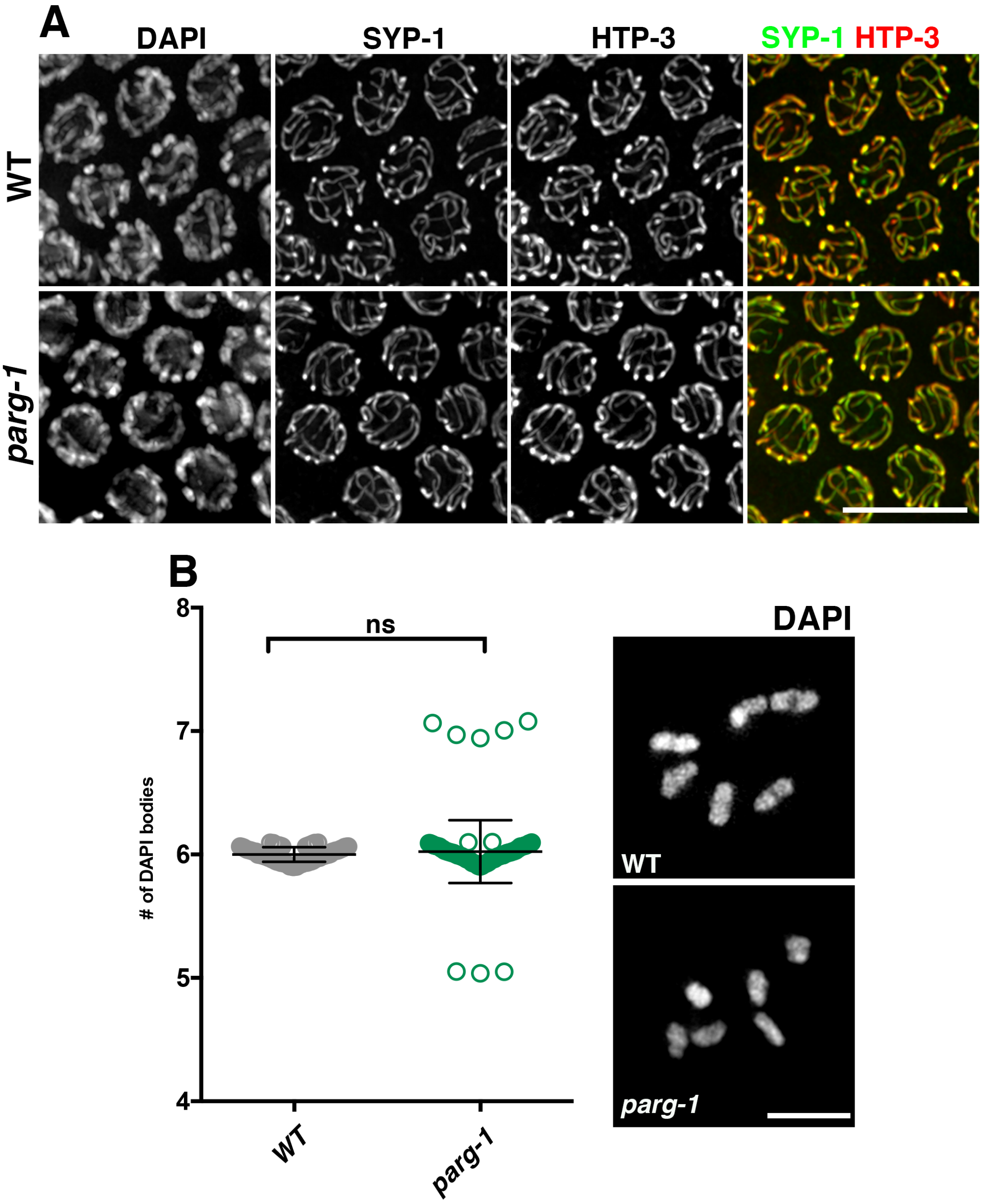

Supplementary Figure 2. PARG-1 is dispensable for synapsis and CO formation. (A) Staining of SYP-1 and HTP-3 shows no abnormalities in *parg-1(gk120)* mutants compared to wild-type (WT) animals. Analysis was performed in biological duplicates. **(B)** Quantification of DAPI-bodies (left) and representative examples (right) of diakinesis nuclei in the indicated genotypes. Scale bar 2 μm. Error bars indicate SD. Statistical analysis was conducted with two-tailed non-parametric Mann-Whitney test (*ns* indicates not significant difference). The number of nuclei analysed was WT (77) and *parg-1(gk120)* (128).

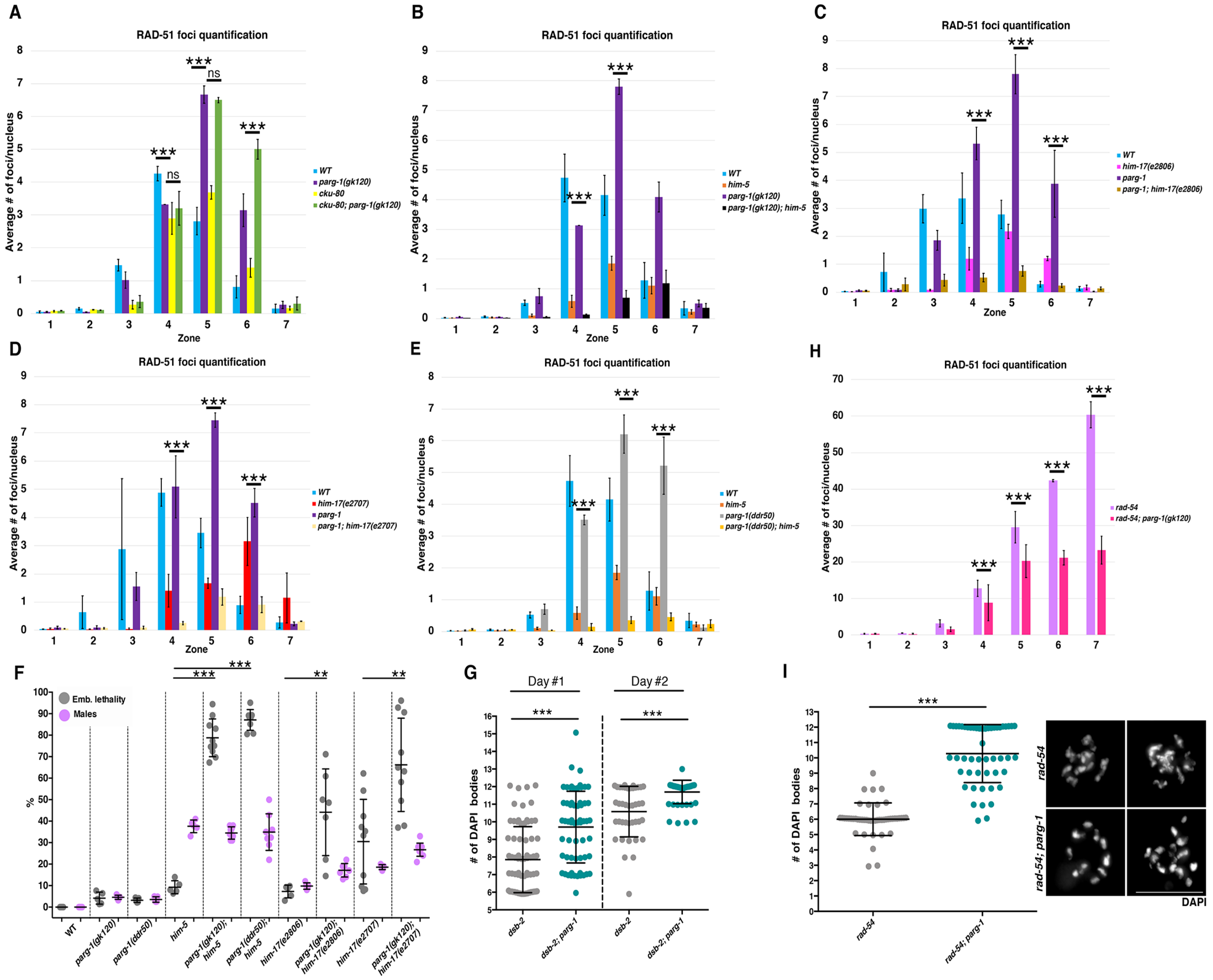

Supplementary Figure 3. Abrogation of *parg-1* function causes reduced amounts of RAD-51 foci in mutants with reduced DSBs and *rad-54*-deficient worms. (A-E) Quantification of RAD-51 foci throughout the germline in the indicated genotypes. Error bars indicate S.E.M. Statistical analysis was performed using non-parametric two-tailed Mann-Whitney test. (****p<0.0001*; *ns= not significant*). **(F)** Removal of *parg-1* causes synthetic lethality in DSB-defective mutants. Error bars indicate SD. (*him-5* vs *parg-1(gk120); him-5*, *p*= 0.0007 - *him-5* vs *parg-1(ddr50); him-5*, *p*= 0.00016 - *him-17(e2806)* vs *parg-1; him-17(e 2806)*, *p*= 0.0025 - *him-17(e2707)* vs *parg-1; him-17(e2707)*, *p*= 0.0015). **(G)** The CO defects in *dsb-2* mutants are exacerbated by lack of PARG-1. Error bars indicate SD.

Statistical analysis was conducted by non-parametric two-tailed Mann-Whitney test (***p<0.0001). **(H)** Abrogation of *parg-1* function reduces RAD-51 foci numbers in the *rad-54* mutant. Error bars indicate S.E.M. Statistical analysis was performed with non-parametric two-tailed Mann-Whitney test. (***p<0.0001). **(I)** Removal of *parg-1* in *rad-54* mutants triggers formation of univalents and largely alleviates chromosome morphology in diakinesis nuclei. Error bars indicate SD. Scale bar 5 μm. Statistical analysis was performed with non-parametric two-tailed Mann-Whitney test. (***p<0.0001).

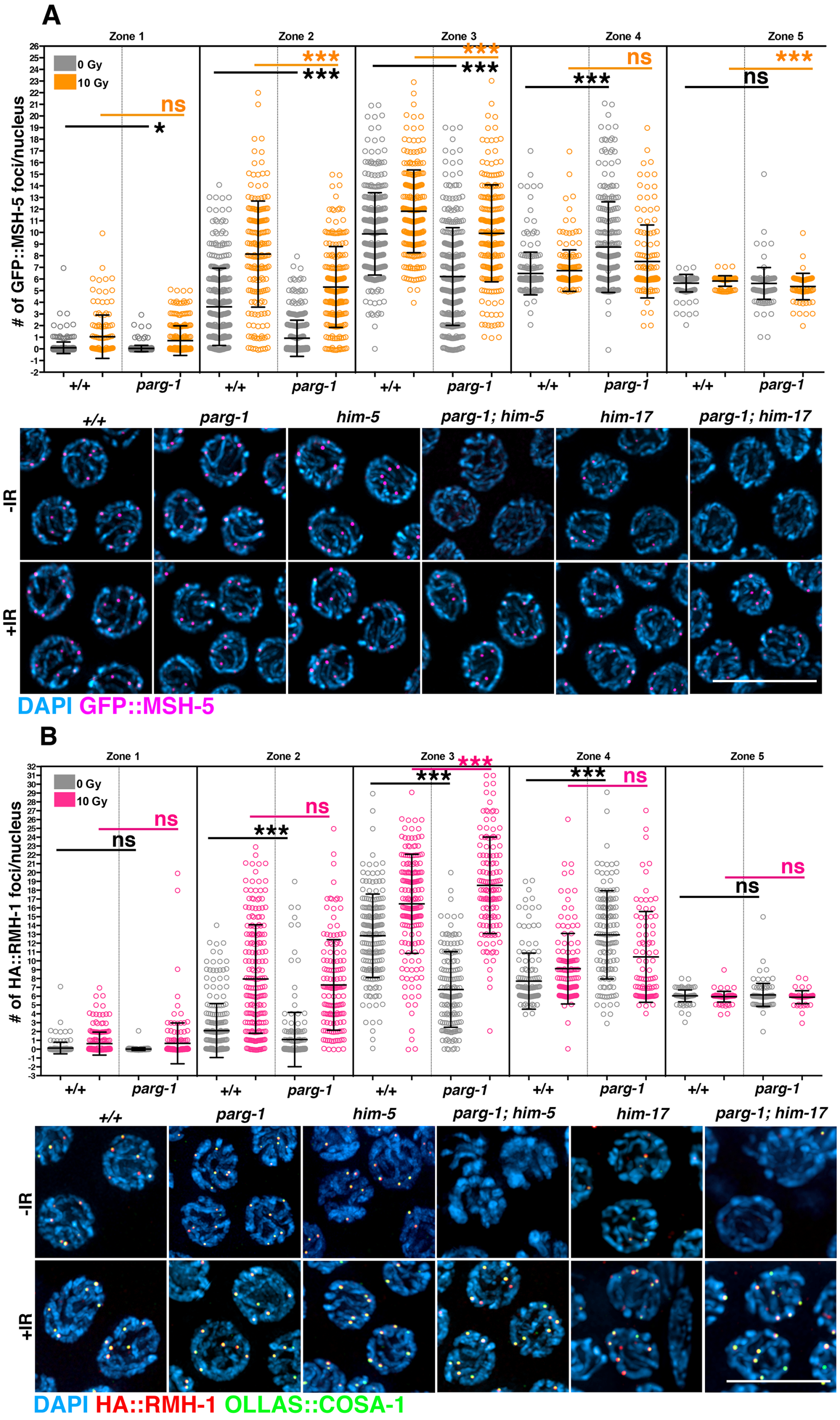

Supplementary Figure 4. Loading of MSH-5 and RMH-1 is delayed in *parg-1* mutants and it is severely impaired in *parg-1; him-5* and *parg-1; him-17* double mutants. (A) Top: quantification of GFP::MSH-5 foci number in controls and *parg-1* mutants. Note that *parg-1* mutants display a delayed accumulation of MSH-5. Bottom: late pachytene nuclei of different genotypes stained for GFP (MSH-5) before and after IR. Scale bar 10 μm. Error bars indicate SD. **(B)** Top: quantification of HA::RMH-1 foci number in controls and *parg-1* mutants. Note that as for MSH-5, *parg-1* mutants display a delayed accumulation of RMH-1 as well. Bottom: late pachytene nuclei of different genotypes stained for HA (RMH-1) and OLLAS (COSA-1) before and after IR. Scale bar 10 μm. Error bars indicate SD. Statistical analysis was performed using non-parametric two-tailed Mann-Whitney test. (***$p<0.0001$; *$p< 0.01$; *ns= not significant*).

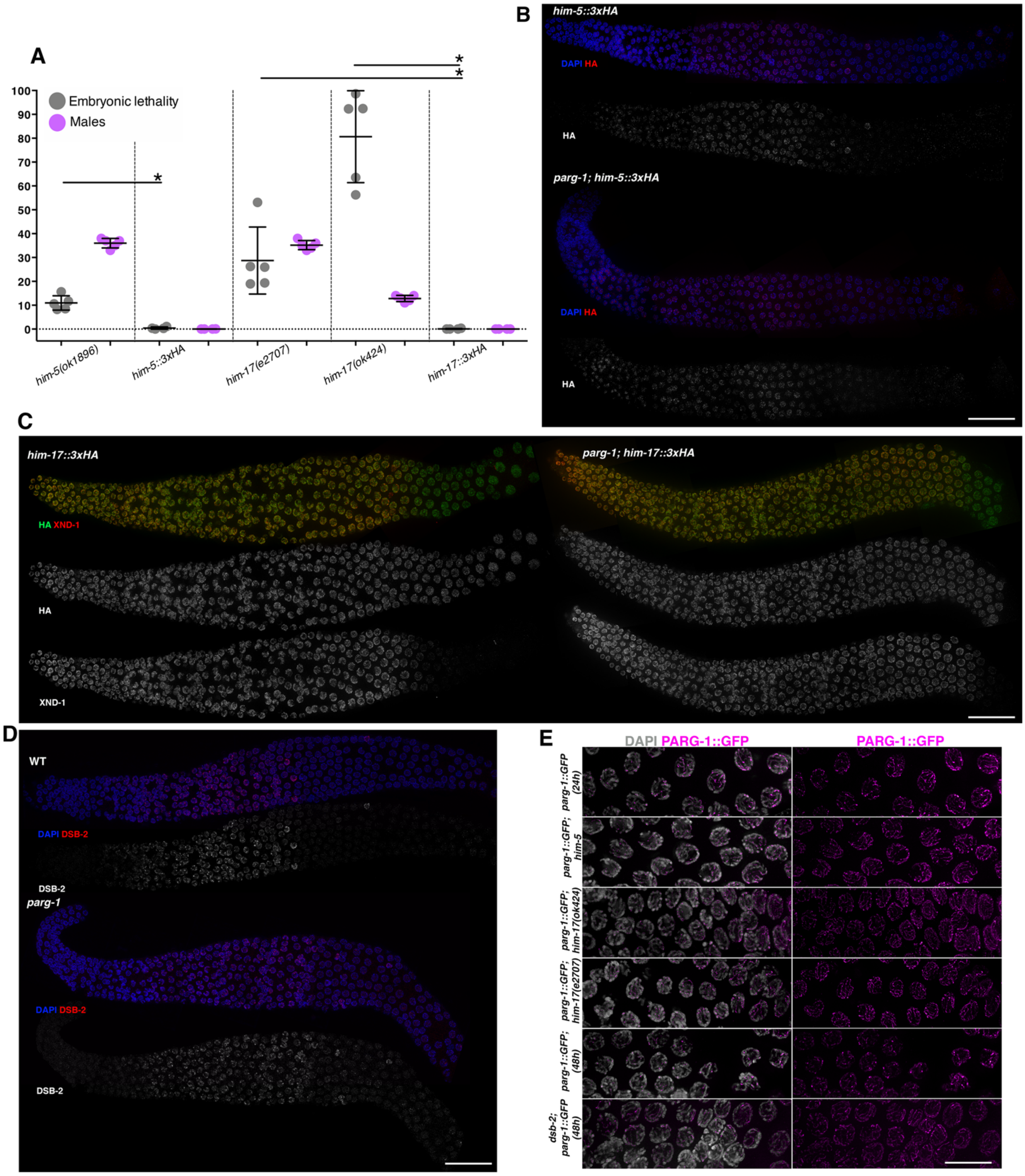

Supplementary Figure 5. PARG-1 and pro-DSB factors display a mutually independent loading. (A) Viability and male progeny assessment revealed full functionality of *him-5::3xHA* and *him-17::3xHA* tagged lines compared to respective mutant backgrounds. Error bars indicate SD. Statistical analysis was performed using non-parametric two-tailed

Mann-Whitney test. (*$p<0.01$). Number of worms scored: *him-5* (5), *him-5::3xHA* (4), *him-17(e2707)* (5), *him-17 (ok424)* (5), *him-17::3xHA* (4). **(B)** HIM-5 shows normal loading in *parg-1* mutant germlines. Scale bar 20 μm. Analysis was performed in biological duplicates. **(C)** HIM-17 and XND-1 do not display loading abnormalities in *parg-1* mutants. Scale bar 20 μm. Analysis was performed in biological duplicates. **(D)** *parg-1* is not required for DSB-2 loading. Scale bar 20 μm. Analysis was performed in biological duplicates. **(E)** Loading of PARG-1 is not dependent on *him-5*, *him-17* and *dsb-2*. Scale bar 20 μm. Analysis was performed in biological duplicates.

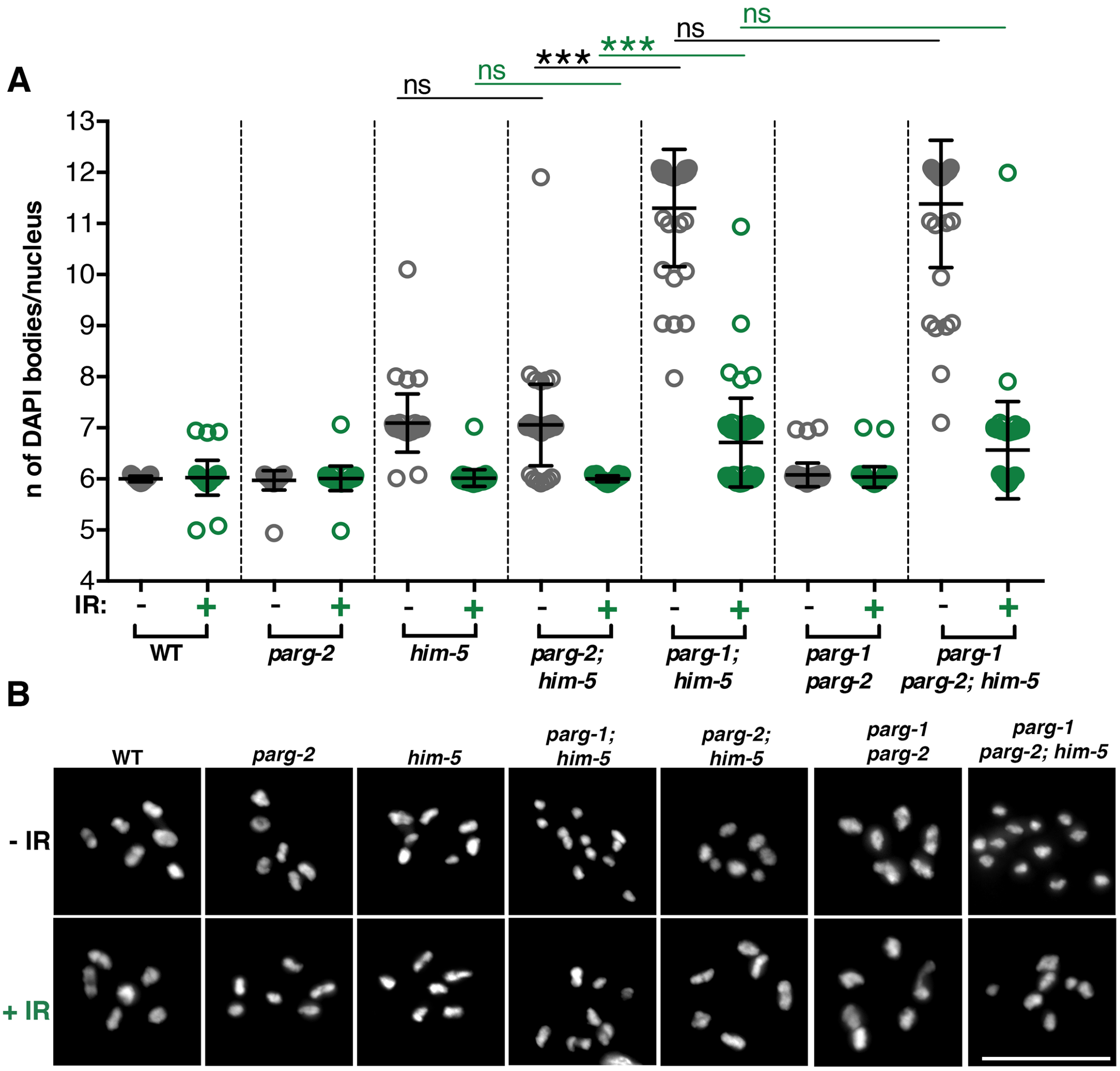

Figure S6. Loss of *parg-2* does not cause synthetic phenotypes with *him-5* irrespectively of *parg-1*. (A) Quantification of DAPI-bodies in diakinesis nuclei of the indicated genotypes before and after IR exposure. Error bars indicate SD. Statistical analysis was performed using non-parametric two-tailed Mann-Whitney test. (****p<0.0001*; *ns= not significant*). Number of nuclei scored is reported in Supplementary Table 2. **(B)** Representative images of diakinesis nuclei of the indicated genotypes stained with DAPI. Scale bar 5 µm.

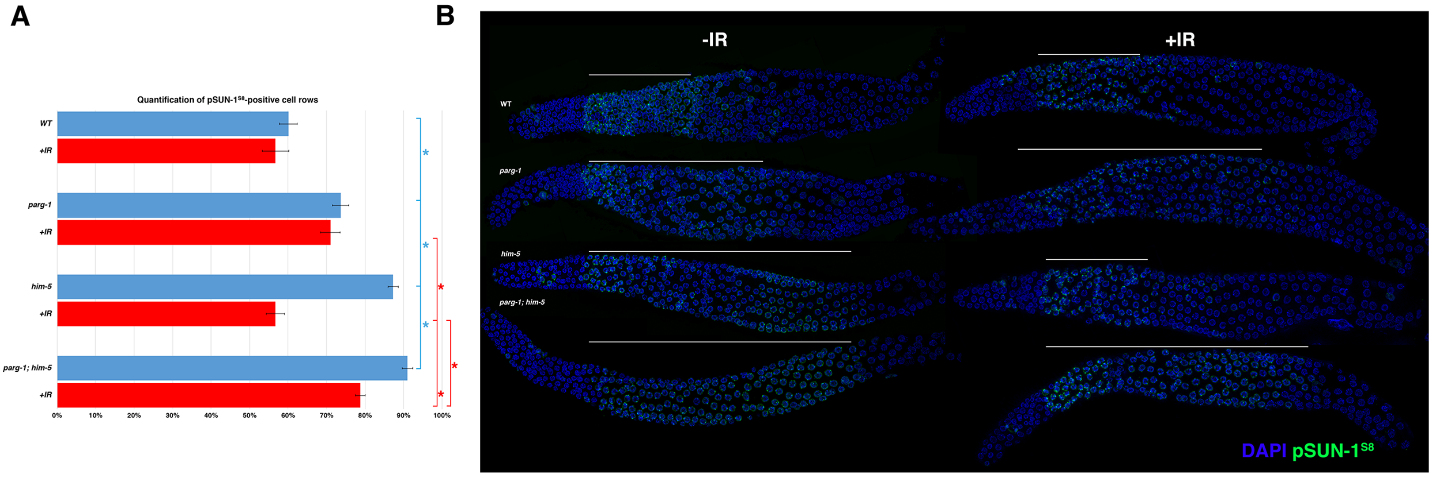

Supplementary Figure 7. IR does not fully suppress accumulation of pSUN-1^{S8} in *parg-1; him-5* double mutants. (A) Quantification of pSUN-1^{S8}-positive nuclei cell rows in the indicated genotypes before and after IR exposure. Error bars indicate S.E.M. Statistical analysis was performed using unpaired *t* test. (**p< 0.01*)**.** Number of gonads analysed (0 Gy-10Gy): WT (4-3), *parg-1* (4-4), *him-5* (3-5), *parg-1; him-5* (5-4). **(B)** Representative whole-mount gonads of the indicated genotypes before and after irradiation, stained for pSUN-1^{S8} and DAPI. Scale bar 30 μm.

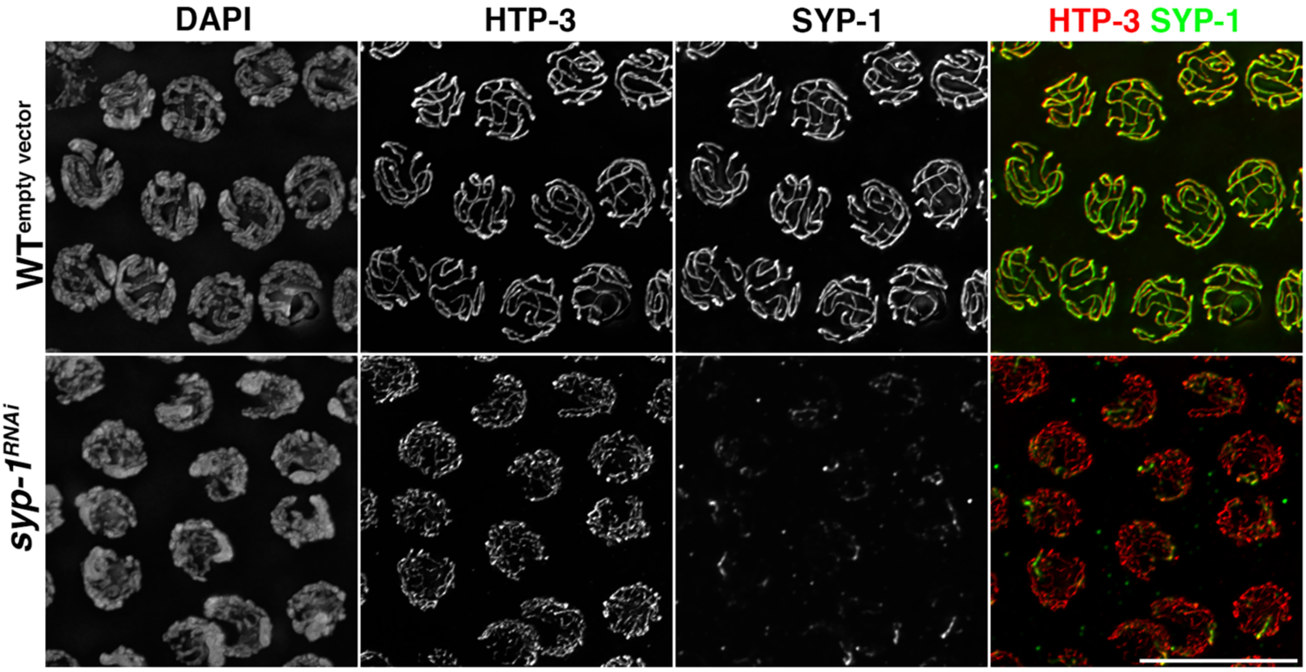

Supplementary Figure 8. Rabbit anti-SYP-1 antibody is specific. Immunostaining analysis in control worms (empty vector) and upon *syp-1RNAi* shows specific detection of SYP-1. Note that SYP-1 is robustly detected along the SC together with HTP-3 but the signal is dramatically reduced under (incomplete) *syp-1RNAi*. Scale bar 10 μm. Analysis was performed in biological duplicates.

Supplementary Table 1.

Number of nuclei analysed for GFP::MSH-5 quantification

Genotype	Zone 1	Zone 2	Zone 3	Zone 4	Zone 5
GFP::msh-5	179	142	159	117	72
GFP::msh-5 +IR	130	170	212	165	105
GFP::msh-5 parg-1	207	178	176	143	58
GFP::msh-5 parg-1 +IR	234	194	211	129	74
GFP::msh-5; him-5	276	239	205	170	107
GFP::msh-5; him-5 +IR	235	246	219	149	82
GFP::msh-5 parg-1; him-5	195	166	141	114	79
GFP::msh-5 parg-1; him-5 +IR	225	202	190	126	63
GFP::msh-5; him-17	379	359	268	215	131
GFP::msh-5; him-17 +IR	181	178	162	100	76
GFP::msh-5 parg-1; him-17	454	417	329	251	230
GFP::msh-5 parg-1; him-17 +IR	182	147	134	84	54

Number of nuclei analysed for HA::RMH-1 quantification

Genotype	Zone 1	Zone 2	Zone 3	Zone 4	Zone 5
HA::rmh-1	196	224	181	153	101
HA::rmh-1 +IR	204	195	171	134	79
HA::rmh-1; parg-1	209	198	148	130	106
HA::rmh-1; parg-1 +IR	174	141	131	87	60
HA::rmh-1; him-5	201	218	172	135	80
HA::rmh-1; him-5 +IR	201	123	118	78	50
HA::rmh-1; parg-1; him-5	209	168	136	89	78
HA::rmh-1; parg-1; him-5 +IR	226	175	141	102	59
HA::rmh-1; him-17	226	207	158	101	85
HA::rmh-1; him-17 +IR	162	144	96	86	68
HA::rmh-1; parg-1; him-17	189	155	138	99	92
HA::rmh-1; parg-1; him-17 +IR	234	215	155	97	75

Supplementary Table 2.

Number of diakinesis nuclei analysed (from Fig. 4)		
Genotype	0 Gy	10 Gy
WT	75	28
parg-1(gk120)	127	43
parg-1(ddr50)	57	56
him-5	85	38
parg-1(gk120); him-5	92	44
parg-1(ddr50); him-5	51	62
him-17(e2806)	161	67
parg-1(gk120); him-17(e2806)	135	94
him-17(e2707)	105	52
parg-1(gk120); him-17(e2707)	119	35
spo-11	49	60
parg-1 spo-11	43	62
Number of diakinesis nuclei analysed (from Fig. 6)		
Genotype	n	-
WT	40	-
parg-1(cd)	56	-
him-5	36	-
parg-1(cd); him-5	42	-
parg-1(gk120); him-5	44	-
parp-1; parg-1(gk120); him-5	33	-
parp-2; parg-1(gk120); him-5	35	-
parp-1; parp-2; parg-1(gk120); him-5	51	-
Number of diakinesis nuclei analysed (from Supp. Fig. 6)		
Genotype	0 Gy	10 Gy
WT	33	40
parg-2	34	40
him-5	44	45
parg-2; him-5	57	53
parg-1; him-5	33	59
parg-1 parg-2	51	53
parg-1 parg-2; him-5	44	49

Supplementary Table 3.

Number of nuclei scored for quantification of OLLAS::COSA-1 foci			
Genotype	0 Gy	10 Gy (8h)	10 Gy (17h)
OLLAS::cosa-1	130	170	118
OLLAS::cosa-1; parg-1	119	101	102
OLLAS::cosa-1; him-5	109	128	156
OLLAS::cosa-1; parg-1; him-5	206	113	132
Number of nuclei scored for quantification of synapsis			
Genotype	0 Gy	10 Gy (8h)	10 Gy (17h)
OLLAS::cosa-1	108	177	149
OLLAS::cosa-1; parg-1	116	112	125
OLLAS::cosa-1; him-5	116	140	184
OLLAS::cosa-1; parg-1; him-5	234	131	160

Supplementary Table 4.

Chromosome I

Genetic Interval / ***Genotype***	**AB**	**BC**	**CD**	**DE**	**EF**	**FG**	**GH**
WT	22.54 (15)	5.9 (4)	13.4 (9)	7.46 (5)	11.94 (8)	7.46 (5)	31.43 (21)
parg-1(gk120)	4.61** (3)	3.07 (2)	29.23** (23)	21.53* (19)	15.38 (12)	3.07 (3)	30.76 (27)
parg-1(cd)	19.54 (17)	8.04 (7)	14.94 (13)	2.29 (2)	9.19 (9)	5.74 (5)	40.22* (35)

The number of COs per interval is shown in brackets. The change in crossover distribution between *wild type* and *parg-1(gk120)* is statistically significant (χ^2 = 51.845, *p< 0.001*). Crossover distribution is not significantly different between wild type and *parg-1(cd)* mutants (χ^2= 6.83, *p= 0.3369*). *, ** refer to statistical significance in recombination frequency within the interval between *wild type* and *parg-1(gk120) (significance level for p<0.05, * p<0.05 - **p<0.001)*

Chromosome V

Genetic Interval / ***Genotype***	**AB**	**BC**	**CD**	**DE**
WT	35.48 (22)	6.45(4)	6.45 (4)	51.61 (32)
parg-1(gk120)	11.84** (19)	15.41* (21)	39.52** (51)	33.54* (50)
parg-1(cd)	28.78 (19)	13.63 (9)	6.06 (4)	51.51 (34)

The number of COs per interval is shown in brackets. The change in crossover distribution between *wild type* and *parg-1(gk120)* is statistically significant (χ^2=234.97, *p< .001*). Crossover distribution is not significantly different between wild type and *parg-1(cd)* mutants (χ^2= 6.0638, *p= 0.1085*). *, ** refer to statistical significance in recombination frequency within the interval between *wild type* and *parg-1(gk120) (significance level for p<0.05, * p<0.05 - **p<0.001)*

Supplementary Table 5

Number of nuclei scored for quantification of RAD-51 foci							
Genotype	Zone 1	Zone 2	Zone 3	Zone 4	Zone 5	Zone 6	Zone 7
WT	222	196	158	137	146	121	117
parg-1	130	170	122	114	105	79	93
spo-11	239	233	218	199	156	155	93
spo-11 parg-1	197	211	200	185	132	102	78
him-5	257	250	182	191	181	145	79
parg-1(gk120); him-5	180	220	177	172	103	153	97
him-17(e2806)	273	233	238	255	254	201	124
parg-1(gk120); him-17(e2806)	199	198	150	126	166	143	88
him-17(e2707)	204	197	171	174	128	78	55
parg-1(gk120); him-17(e2707)	172	189	154	135	107	80	78
parg-1(ddr50)	196	226	158	153	145	136	102
parg-1(ddr50); him-5	208	257	188	175	156	115	88
rad-54	137	167	109	97	99	87	83
rad-54; parg-1	129	181	157	107	90	72	69
cku-80	136	254	219	208	184	166	149
cku-80; parg-1(gk120)	207	277	206	181	141	116	116

Supplementary Table 6.

Genotype	**Source**	**Id. number**
parp-1(ddr31) I.	This study	NSV167
rmh-1(jf172[HA::rmh-1]) I.	This study	NSV240
htp-3::TEV::eGFP::myc::3xFLAG I.	CGC	JH4008
rad-54(tm1268)/hT2[bli-4(e937) let-?(q782) qIs48] (I;III)	Jantsch lab	NSV187
parp-2(ok344) II.	CGC	VC1171
dsb-2(me96) II.	Villeneuve lab	AV477
GFP::cosa-1 II.	Villeneuve lab	AV630
cosa-1(tm3298)/qC1[dpy-19(e1259) glp-1(q339) qIs26] III.	Villeneuve lab	AV590
oxTi574 II; unc-119(ed3) III.	CGC	EG7875
cosa-1(ddr12[OLLAS::cosa-1]) III.	Janisiw et al.; 2018	NSV97
parg-1(gk120) IV.	CGC	VC130
parg-1(ddr50) IV.	This study	NSV277
parg-2(ddr20) IV.	This study	NSV140
parg-1(ddr3[parg-1::GFP]) IV.	This study	NSV25
parg-1(gk120) parg-2(ddr20) IV.	This study	NSV126
msh-5(ddr22[GFP::msh-5]) IV	Janisiw et al.; 2018	NSV129
parg-1(ddr29[parg-1^{E554,555A}*::GFP]) IV.*	This study	NSV162
parg-1(ddr34[parg-1^{E554,555A}*]) IV.*	This study	NSV177
parg-1^{gk120}*(ddr51) IV in CB4856.*	This study	NSV278
him-5(ok1896) V.	CGC	RB1562
him-17(e2806) V.	This study	NSV169
him-17(e2707) V.	This study	NSV170

him-17(ddr37[him-17::3xHA]) V.	This study	NSV205
syp-2(ok307)7nT1 [unc-?(n754) let-?(m435)] (IV;V).	CGC	AV276
parp-2 (ok344) II; parg-1(gk120) IV.	This study	NSV09
spo-11(ok79)/nT1 [unc-?(n754) let-?] (IV;V).	CGC	AV106
syp-3(ok758) I; ieSi11 II; unc-119(ed3) III.	CGC	CA1218
parg-1(gk120) IV; him-5(ok1896) V.	This study	NSV56
parg-1(gk120) spo-11(ok79)/nT1 [unc-?(n754) l et-?] (IV;V).	This study	NSV74
parg-1(gk120) with Hawaiian chromosome V	This study	NSV121
parg-1(ddr3[parg-1::GFP]) IV; him-5(ok1896) V.	This study	NSV124
cosa-1(ddr12[OLLAS::cosa-1]) III; parg- 1(gk120) IV.	This study	NSV137
cosa-1(ddr12[OLLAS::cosa-1]) III; him- 5(ok1896) V.	This study	NSV138
cosa-1(ddr12[OLLAS::cosa-1]) III; parg- 1(gk120) IV; him-5(ok1896) V.	This study	NSV139
cku-80(ok861) III.	CGC	RB964
cosa-1(ddr12[OLLAS::cosa-1]) III; parg- 1(gk120); him-5(ok1896)/nT1[unc-?(n754) let-?] (IV	This study	NSV155
parg-1(gk120) msh-5(ddr22[GFP::msh-5]) IV	This study	NSV157
parg-1(ddr3[parg-1::GFP]) IV; syp- 2(ok307)7nT1 [unc-?(n754) let-?(m435)] (IV;V).	This study	NSV160
dsb-2(me96) II; parg-1(gk120) IV.	Yanowitz lab	QP1367
mre-11(iow1)/nT1 [qIs51] (IV;V).	CGC	SSM2
parg-1(gk120) IV; him-17(e2806) V.	Yanowitz lab	QP1374
parg-1(gk120) IV; mre-11(iow1)/nT1 [qIs51] (IV;V).	Yanowitz lab	QP1377
parp-1(ddr31) I; parp-2(ok344) II.	This study	NSV175
parg-1(ddr34[parg-1^{E554,555A}*]) IV in CB4856.*	This study	NSV178
rmh-1(jf54)/ hT2 [bli-4(e937) let-?(q782) qIs48] (I;III).	This study	NSV180
parg-1(ddr34[parg-1^{E554,555A}*::GFP]) IV; him- 5(ok1896) V.*	This study	NSV181
com-1(t1626) unc-32(e189)/hT2 [bli-4(e937) let- ?(q782) qIs48] (I;III).	This study	NSV182
parp-1(ddr31) I; parg-1(gk120) IV.	This study	NSV184
cosa-1(tm3298)/qC1[dpy-19(e1259) glp- 1(q339) qIs26] III; parg-1(ddr3[parg-1::GFP]) IV.	This study	NSV186
parg-1(ddr34[parg-1^{E554,555A}*]) IV; him-5(ok1896) V.*	This study	NSV190
com-1(t1626) unc-32(e189)/hT2 [bli-4(e937) let- ?(q782) qIs48] (I;III); parg-1(gk120) IV.	This study	NSV194
him-17(ok424)/nT1 [unc-?(n754) let-?] (IV;V).	This study	NSV196
parp-1(ddr31) I; parp-2(ok344) II; parg-1(gk120) IV.	This study	NSV199
parg-1(gk120) IV; him-17(ddr37[him-17::3xHA] V.	This study	NSV206
parg-1(gk120)/nT1 [unc-?(n754) let-?] (IV;V).; him-17(ok424)/nT1 [unc-?(n754) let-?] (IV;V).	This study	NSV209

parg-1(gk120)/nT1 [unc-?(n754) let-?] (IV;V).; him-17(e2707)/nT1 [unc-?(n754) let-?] (IV;V).	This study	NSV236
msh-5(ddr22[GFP::msh-5]) IV; him-5(ok1896) V.	This study	NSV241
msh-5(ddr22[GFP::msh-5]) IV; him-17(e2707) V.	This study	NSV242
parp-2(ok344) II; parg-1(gk120) IV; him- 5(ok1896) V.	This study	NSV244
him-17(e2707)/nT1 [unc-?(n754) let-?] (IV;V).	This study	NSV246
msh-5(ddr22[GFP::msh-5])/nT1 [unc-?(n754) l et-?] (IV;V); him-17(e2707)/nT1 [unc-?(n754) let-?] (IV;V).	This study	NSV247
him-5(ddr43[him-5::3xHA]) V.	This study	NSV250
parg-1(gk120) IV; him-5(ddr43[him-5::3xHA]) V.	This study	NSV252
rmh-1(jf172[HA::rmh-1]); cosa- 1(ddr12[OLLAS::cosa-1]) III; parg-1(gk120) IV.	This study	NSV253
parg-1(gk120) msh-5(ddr22[GFP::msh-5])/nT1 [unc-?(n754) let-?] (IV;V); him-17(e2707)/nT1 [unc-?(n754) let-?] (IV;V).	This study	NSV254
htp-3(tm3655)/hT2 [bli-4(e937) let-?(q782) qIs48] (I;III).	This study	NSV255
rmh-1(jf172[HA::rmh-1]); cosa- 1(ddr12[OLLAS::cosa-1]) III; him-5(ok1896) V.	This study	NSV256
rmh-1(jf172[HA::rmh-1]); cosa-1(ddr12[OLLAS::cosa-1]) III; parg-1(gk120) IV; him- 5(ok1896) V.	This study	NSV257
rmh-1(jf172[HA::rmh-1]) I; cosa- 1(ddr12[OLLAS::cosa-1]) III.	This study	NSV258
parg-1(ddr3[parg-1::GFP]) IV; him-5(ddr43[him- 5::3xHA]) V.	This study	NSV262
htp-3(tm3655)/hT2 [bli-4(e937) let-?(q782) qIs48] (I;III); parg-1(ddr3[parg-1::GFP]) IV.	This study	NSV265
parg-1(ddr3[parg-1::GFP]) IV; him- 17(ddr37[him-17::3xHA]) V.	This study	NSV267
parg-1(gk120) msh-5(ddr22[GFP::msh-5]) IV; him-5(ok1896) V.	This study	NSV273
rmh-1(jf172[HA::rmh-1])I; cosa- 1(ddr12[OLLAS::cosa-1]) III; him-17(e2707) V.	This study	NSV276
dsb-2(me96) II; parg-1(ddr3[parg-1::GFP]) IV.	This study	NSV280
parg-1(ddr3[parg-1::GFP]) IV; him-17(e2707) V.	This study	NSV281
rmh-1(jf172[HA::rmh-1]) I; cosa- 1(ddr12[OLLAS::cosa-1]) III; parg-1(gk120)/nT1 [unc- ?(n754) let-?] (IV;V); him-17(e2707)/nT1 [unc-?(n754) let-?] (IV;V).	This study	NSV286
cosa-1(ddr12[OLLAS::cosa-1]) III; parg- 1(ddr3[parg-1::GFP]) IV.	This study	NSV292
parg-1(ddr3[parg-1::GFP])/nT1 [unc-?(n754) l et-?] (IV;V); him-17(ok424)/nT1 [unc-?(n754) let-?] (IV;V).	This study	NSV294

List of primers used in the study.

Primers Name	Sequences	Amplicone
PR185 PR186	5´-CCGTCACGACAAAATGCAGA-3´ 5´-TGCCACCTTCTCCAATGACT-3´	*parp-1(ddr31)* *Deletion only*
PR301 PR302	5´-ACAGAGTACCACTTCACCTTTCC-3´ 5´-AATGCAACTTTTACTGCGCTCG-3´	*HA::rmh-1*
PR305 PR306	5´-GCCTGCCATAGAACCACCTG-3´ 5´-GGCGTCGCGACCTCTAGAAA-3´	*rad-54(tm1268)*
PR011 PR012	5´-CGAGAAAACTCATCTTCATTG-3´ 5´-AAAGGATTAGCAACACCTTCAGA-3´	*parp-2(ok344)*
PR100 PR101	5´-CAATGTCAAGTTCTCGGTGA-3´ 5´-AAAATTTGCGAAAAATGGTC-3´	*cosa-1(tm3298)*
PR55 PR56	5´-ACTTTGTATTGGTCTCGCAC-3´ 5´-AACCTGATTCGCTGCTGATA-3´	*OLLAS::cosa-1*
PR005 PR006	5´-ATTTTGACAAGGCGAGAGGA-3´ 5´-CGAGCTTACGTTTGATGCTT-3´	*parg-1(gk120)* *deletion only*
PR021 PR022	5´-GATTGCATTTACTGAGGGAAA-3´ 5´-CATGATTTTCAACTGTGACCA-3´	*parg-1(gk120)* *N2 only*
PR027 PR028	5´-AAATGTAGAGCGAGATTTTG-3´ 5´-TGAAATGGTCATGATCAGTT-3´	*parg-2(ddr20)*
PR205 PR206	5´-TGCTAACTTACAGGCATGCT-3´ 5´-TGCATGGATTGGTTTCACAC-3´	*parg-1::GFP*
PR33 PR34	5´-GTTTTTCAGCAACCTTTTCTT-3´ 5´-ATTATCATCACGGGGTAAGG-3´	*GFP::msh-5*
PR154 PR155	5´-TGTGGAGAAACTTAAATTCCTGT-3´ 5´-TCGCTTCCAGTTGTTTCATTT-3´	*parg-1(cd) digested with AluI*
PR220 PR221	5´-CGGAGCTCAAAATGAAAAGAGCAGC-3´ 5´-CGATGCGACCAACTGTTTTTCG-3´	*him-5(ok1896)*
PR199 PR200	5´-TGGAGGGAGAAGAAGAAGAAGT-3´ 5´-TCAGAAACAACGCAACGAATT-3´	*him-17::3xHA*
PR45 PR46	5´-AGAGTCAGCTTCGCATCTCC-3´ 5´-AAAAGGAAACTACGCCATCG-3´	*syp-2(ok307)*
PR75 PR76	5´-CGTGGAAACATTGCTTGAAA-3´ 5´-GGACTGATGGAACCGAGAAA-3´	*spo-11(ok79)*
PR203 PR204	5´-TTCGATGCCATACACCTTCA-3´ 5´-TCAAAGTCATCCGAATCTATTGG-3´	*him-17(ok424)*
PR102 PR103	5´-GACTGTTTTCCAGGCGTAAA-3´ 5´-AATTACCCTTTTTGGGTTCA-3´	*htp-3(tm3655)*
PR228 PR229	5´-TGAACAGTCACAGGAAATCAC-3´ 5´-AGTTATATGCCCGAGTGTCC-3´	*him-5::3xHA*
I, -19	5´-ATGCCAGTGATAAGGAACGG-3´ 5´-TCACATCCCTTGTCGATGAA-3´	snp_F56C11
I, -12	5´-TCGAAATCAGGGAAAAATTGA-3´ 5´-ACGATTTTCGGGGAGTTTTT-3´	snp_Y71G12
I, -6	5´-GTTTTCACTTTTGCCGGTGT-3´ 5´-TGAAGGCGCATATACAGCAG-3´	pkP1052
I, -1	5´-AAAATATCAGGAAAGAGTTTCGG-3´ 5´-TTTAAAGATTAAGGGTGGAGCG-3´	snp_D1007
I, 5	5´-ATCTGGCACCAAATATGAGTCG-3´ 5´-AATCTCGATTTTCAAGGAGTGG-3´	CE1-247
I, 13	5´-TCCTGGATAATCCCCAAAAA-3´	snp_F58D5

	5´-CCCTGCCATTGATCTTGTTT-3´	
I, 14	5´-TTGAAATCCCCTTTAAAATCCC-3´ 5´-ACACTGGGTACCTGACTCATGC-3´	uCE1-1361
I, 26	5´-ATTATTAACGGCCACGGTGA-3´ 5´-CCCACACACTCTCACCTTCA-3´	snp_Y105E8B
V, -17	5´-TTTCGGAAAATTGCGACTGT-3´ 5´-CGCGTTTTGGAGAATTGTTT-3´	pkP5076
V, -5	5´-GAGATTCTAGAGAAATGGACACCC-3´ 5´-AAAAATCGACTACACCACTTTTAGC-3´	snp_Y61A9L
V, 1	5´-AGAAATGATCCGATGAAAAAGC-3´ 5´-CCGATAGTGTTCATAGCATCCC-3´	pkP5097
V, 6	5´-CAAATTAAATATTTCTCAAAGTTTCGG-3´ 5´-ACATAAGCGCCATAACAAGTCG-3´	R10D12
V, 18	5´-GAAATTCAAATTTTTGAGAAACCC-3´ 5´-TTCAGACCATTTTTAGAATATTCAGG-3´	snp_Y17D7B

Uncropped blots from Figure 2

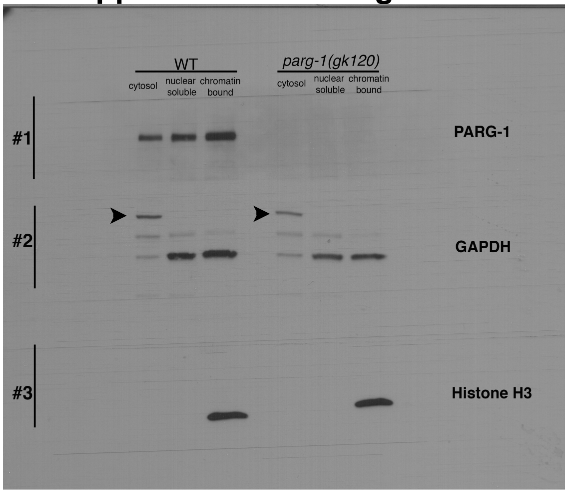

Fig. 2a

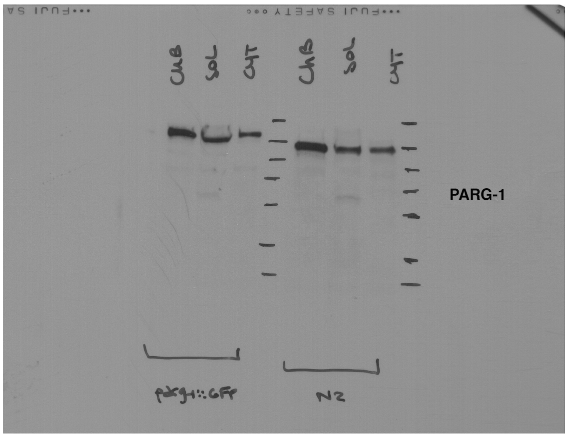

Fig. 2b

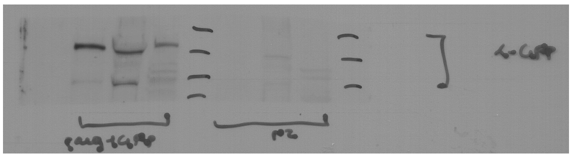

Fig. 2b

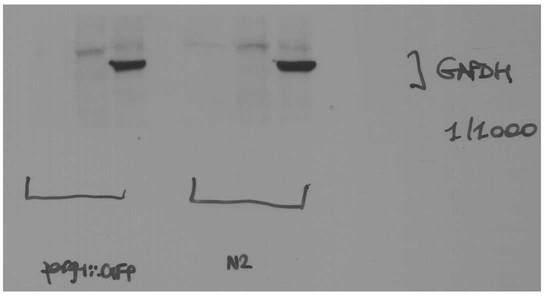

Fig. 2b

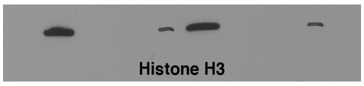

Fig. 2b